
FINANCIAL TIME SERIES DATA AUGMENTATION WITH GENERATIVE ADVERSARIAL NETWORKS AND EXTENDED INTERTEMPORAL RETURN PLOTS

Justin Hellermann

School of Business and Economics
Humboldt University of Berlin
Berlin

justin.hellermann@hu-berlin.de

Qinzhuan Qian

IT Engineer ING
ING Bank N.V.
Amsterdam

phyllis.qian@mendesgans.nl

Ankit Shah

Senior IT Chapter Lead ING
ING Bank N.V.
Amsterdam

ankit.shah@ing.com

ABSTRACT

Data augmentation is a key regularization method to support the forecast and classification performance of highly parameterized models in computer vision. In the time series domain however, regularization in terms of augmentation is not equally common even though these methods have proven to mitigate effects from small sample size or non-stationarity. In this paper we apply state-of-the-art image-based generative models for the task of data augmentation and introduce the extended intertemporal return plot (XIRP), a new image representation for time series. Multiple tests are conducted to assess the quality of the augmentation technique regarding its ability to synthesize time series effectively and improve forecast results on a subset of the M4 competition. We further investigate the relationship between data set characteristics and sampling results via Shapley values for feature attribution on the performance metrics and the optimal ratio of augmented data. Over all data sets, our approach proves to be effective in reducing the return forecast error by 7% on 79% of the financial data sets with varying statistical properties and frequencies.

Keywords Data Augmentation · Generative Adversarial Networks · Time Series · Extended Intertemporal Return Plots · XIRP · Intertemporal Return Plots · IRP · Shapley Values

1 Introduction

Augmenting image data has become a fundamental part of many machine learning pipelines and is a widely applied regularization technique to improve model robustness and performance (Geron, 2017, p. 309). In the computer vision community these techniques magnify the number of training examples by scaling, rotating and shifting images. This allows for running multiple training epochs on variations of the same underlying image.

Even though time series also face the challenge of limited training examples, the application of data augmentation methods is not equally common. In the classic, parametric setting, data augmentation is not per se required, since the models have few parameters to fit. Nevertheless, this changes quickly, once more complex neural network based models have to be trained. But data augmentation has more far-reaching benefits than solely allowing to train highly parameterized models. Expanding the amount of train data can improve the performance of regression and classification tasks, analogously to the improved estimates via bootstrapping techniques. In physics and system engineering the benefit of time series augmentation is established and applied successfully to enlarge existing train data (Theiler et al., 1992). This partly results from the characteristics of time series in the context of system engineering which often exhibit less randomness compared to economic and financial data sets.

For decades, data augmentation therefore remained in the area of physics before moving into finance (Le Guennec et al., 2016; Ziyin et al., 2021). Just recently, researchers began to apply data augmentation methods to financial time series trying to mitigate the effects of random and noisy features, sudden jumps and nonstationary. Since many nonparametric time series models need increased amounts of data to generalize well, augmenting existing time series is promising to boost performance, as shown by Yuan et al. (2020); Lee and Kim (2020). In this paper we consider different financial

data sets and introduce an extended version of the IRP to create image representations encoding both the time series as well as intertemporal returns. Combining the new image representation with advanced generative models facilitates the augmentation of time series data. The new approach is tested on a large number of financial datasets with varying frequencies spanning from daily to yearly data. A series of test is conducted in and among the different data frequencies to answer the following research questions: i) Can forecasting models benefit from augmented data and if so to what extent? ii) What is the optimal ratio between real and augmented data? iii) Which statistical properties contribute to a successful augmentation?

2 Related Work

Since the proposed approach combines generative models, image representations of time series and data augmentation, we discuss related work at different topical intersections. The related work mainly focuses on time series data augmentation methods and its the benefits as well as an introduction to other time series image representations.

Data augmentation for the purpose of classification has been applied by Forestier et al. (2017), who use dynamic time warping barycentric averaging to produce new samples. A more complex approach is chosen by Le Guennec et al. (2016), who use a deep convolutional neural network architecture to generate synthetic data for time series classification. For time series forecasting many models rely on transformation and bootstrapping methods Iftikhar et al. (2017); Bergmeir et al. (2016); Bandara et al. (2021). Bergmeir et al. (2016) use repeated sampling techniques to improve forecasts by aggregation (bagging) of exponential smoothing methods. By separating the time series into the trend, seasonal part, and remainder bagging using Box–Cox transformation and STL decomposition, their approach returned promising results for monthly economic data. The related concept of IAAFT by Schreiber and Schmitz (2000) combines the bootstrap approach with shuffling time series which have been generated by Fourier transform to simulate new time series. From the area of parametric simulations Denaxas et al. (2015); Papaefthymiou and Klockl (2008) apply Markov Chain Monte Carlo methods to simulate and thereby augment time series data. Another recent approach named GRATIS by Kang et al. (2020), use mixture autoregressive models to generate time series with diverse and controllable features. According to the authors, the main benefit lies in a more reliable model selection due to the possibility to test on an extended amount of data. Apart from mixture autoregressive models which require assumptions on the underlying process, the non-parametric class of GAN architectures, especially the one proposed by Karras et al. (2020), have received significant attention, as a result of their outstanding successes in generating new images. The successes of the adversarial methods were also partly transferred to the domain of time series to synthetic data (Fu et al., 2019; Yoon et al., 2019; Esteban et al., 2017; Zhang et al., 2015)

Studies regarding the augmentation benefit for forecasting are sparsely covered. Bandara et al. (2021) evaluated the GRATIS and Moving Block Bootstrapping, Dynamic Time Warping Barycentric Averaging techniques to improve the accuracy of global forecasting models. Smyl and Kuber (2016) examine multiple time series augmentation methods (Markov Chain Monte Carlo, local-global-trend algorithm, exponential smoothing) for multiple short time series forecasting with recurrent neural networks.

Related image representations are Gramian Angular Summation and Gramian Angular Difference Fields (Wang and Oates, 2014), which rely on a polar encodings their inverse trigonometric function to the sum or the difference of the encoding. Also Waveforms are often used to encode the shape of a time series graph as a function of time. Gramian Angular Fields, Waveforms and recurrence plots rely on a deterministic encodings of a time series. A different approach is chosen by Markov transition fields as applied by Wang and Oates (2014) to bin the time series in different classes and then calculate transition probabilities and represent them in a two dimensional space. Also spectrograms rely on a probabilistic encoding and have been applied successfully in processing audio signals and visualizing the spectrum of frequencies of a signal as it varies with time (Wyse, 2017) while each plot is characteristic for a certain sound or a spoken word. Depending on the approach of encoding, some of the upper methods are limited in their applications and can either recover the initial time series only partially or approximately.

This paper complements the existing studies by two novel aspects. First, the paper introduces a new image representation named XIRP and then trains an image-based GAN to augment the existing data. Further, we apply Shapley values for model explainability to get an improved insight into what factors contribute to each of the performance metrics. The ensemble of Shapley values and image-based generative models for time series is, to the best of our knowledge, not yet covered in the literature.

3 Methodology

In this paper we use a Wasserstein GAN which is an extension of the vanilla GAN by Goodfellow et al. (2014). The vanilla GAN consists a generator network G and a discriminator network D with opposing objective functions. In the course of training, G generates a fake distribution \tilde{x} and proposes it to D , which assesses the likelihood of \tilde{x} originating

from the true data distribution. The adversarial game between G and D can be described by the objective function

$$\min_G \max_D \mathbb{E}_{x \sim \mathbb{P}_r} [\log(D(x))] + \mathbb{E}_{\tilde{x} \sim \mathbb{P}_g} [\log(1 - D(\tilde{x}))] \quad (1)$$

where D and G try to maximize and minimize (3), respectively. $D(x)$ is the estimate of the discriminator that x is real while \mathbb{P}_r denotes the real data distribution. The generated data is denoted by \tilde{x} with $\tilde{x} = G(z)$ and $z \sim p(z)$ where p denotes some distribution, such as uniform or Gaussian. \mathbb{P}_g is the distribution of the generated data, or, put differently, the model distribution. Having the opposing objectives, both networks play an iterative game and train each other in the process. The above vanilla GAN suffers from stability problems and is difficult to train (Goodfellow et al., 2014). Arjovsky et al. (2017) address this problem by proposing a Wasserstein-GAN (WGAN) with a more stable training behavior including correlation between the value of the objective function and sample quality. An intuitive explanation for the Wasserstein distance as a loss function can be obtained from its synonym *Earth Mover Distance*. It can be related to the minimum cost of transporting mass in order to transform the distribution q into the distribution p , whereby the cost is mass times transport distance. The Wasserstein metric changes the upper objective function to

$$\min_G \max_{D \in \mathcal{D}} \mathbb{E}_{x \sim \mathbb{P}_r} [D(x)] - \mathbb{E}_{\tilde{x} \sim \mathbb{P}_g} [D(\tilde{x})] \quad (2)$$

where \mathcal{D} is defined as a set of 1-Lipschitz functions and \hat{x} is a randomly sampled subset. Instead of classifying generated images as real or fake, the WGAN replaces the discriminator model by a critic that scores the realness or fakeness of an image. Gulrajani et al. (2017) further improve training in their WGAN-GP, which incorporates gradient penalty terms for the discriminative network. This changes the objective function to

$$\min_G \max_{D \in \mathcal{D}} \mathbb{E}_{x \sim \mathbb{P}_r} [D(x)] - \mathbb{E}_{\tilde{x} \sim \mathbb{P}_g} [D(\tilde{x})] + \lambda \mathbb{E}_{\tilde{x} \sim \mathbb{P}_{\hat{x}}} [(\|\nabla_{\tilde{x}} D(\hat{x})\|_2 - 1)^2] \quad (3)$$

The gradient penalty term $[(\|\nabla_{\tilde{x}} D(\hat{x})\|_2 - 1)^2]$ opposes vanishing and exploding gradients. We refer to Gulrajani et al. (2017) for a more detailed explanation of all underlying concepts and considerations. In this paper, G is trained on an extended version of IRPs recently proposed by Hellermann and Lessmann (2021). The concept of IRPs mixes insights from quantitative finance with the idea recurrence plots by Eckmann et al. (1987). It calculates returns between all points in a time series returning an $N \times N$ representation of a time series with length N . The IRP with indexes i and j is obtained by calculating the pairwise logarithmic return

$$R_{i,j}^C = \log \left(\frac{x_i}{x_j} \right) \quad \forall i, j \in \{1, 2, \dots, S\} \quad (4)$$

Once the start value at $t = 0$ is known, any time series can be recovered from the IRP regardless whether it is a real or simulated representation. Note, that $x \in \mathbb{R}_+$ must be ensured by scaling since returns must be calculated on positive values.

Since we want to compare augmentation techniques that do not sample returns but a scaled time series an extension is required. A careful look at the IRP reveals that in case $i = j \implies R_{i,j}^C = 0$ which leads to a diagonal filled with zeros. This motivates the formulation to the extended IRP (XIRP) which complements the intertemporal return structure by adding extra information to the encoding. Thus, equation (4) can be written as:

$$R_{i,j}^X = \begin{cases} \log \left(\frac{x_i}{x_j} \right) & \forall i, j \in \{1, 2, \dots, S\} \wedge i \neq j \\ x_i & \forall i, j \in \{1, 2, \dots, S\} \wedge i = j \end{cases} \quad (5)$$

The advantages of the approach are manifold. First, the diagonal of the IRP does not contain any information and is filled with additional feature in the XIRP. Second, we can directly compare the results to other sampling techniques without rescaling and calculating returns for the object of comparison. Since the diagonal of the XIRP contains an additional feature, a joint scaling would suggest a single feature and affect results negatively. As a result, the diagonal and the off-diagonal have to be scaled independently. Linking the concepts of GAN and XIRP we can now sample and extract the time series from the diagonal while the returns are saved in the off-diagonal. There are multiple ways of recovering a time series from an XIRP. Since the initial values are stored in the diagonal, these can be directly extracted, ignoring all off-diagonal information encoded in the data. However, this would neglect parts of the encoded information thus we propose to extract the diagonal in a first step and then use the diagonal as a baseline time series to calculate variants. This involves replacing the diagonal of the initial XIRP with $d_{ij}^{XIRP} = 1 \quad \forall i, j \in \{1, 2, \dots, S\}$. Afterwards, the extracted diagonal can be multiplied column-wise with the $XIRP_{d=1}$, so that S time series are obtained which consider the dynamics encoded in the off-diagonal. An additional option is to average over the S time series or randomly pick one of them. Randomly choosing a single instance or averaging over all time series are valid methods to obtain a single time series. Thus, the approach can be used as a scale-invariant encoding and also as an encoding for the raw time series.

In order to identify the contributing factors for a successful augmentation we make use of the concept of Shapley Values. Invented as a solution mechanism for cooperative behavior in game theory by Shapley (1951), it has become popular for explaining the contribution of features to a prediction and is now frequently used to enhance model understanding (Ghorbani and Zou, 2019; Merrick and Taly, 2020; Antipov and Pokryshevskaya, 2020). To quantify the feature importance, these are successively added in a random order and the contribution to the prediction is calculated. The Shapley value of a feature value is the average change in the prediction that results from the new feature having joint. Its ability to explain the predictions of nonlinear models along with its desirable properties make it a competitive alternative to more complex models such as Layer-Wise Relevance Propagation or Locally Interpretable Model-Agnostic Explanations (LIME). Please refer to Shapley (1951) for a detailed introduction to the concept, its variants and considerations.

4 Data and Test Design

For the upcoming series of tests we use financial data with varying frequencies from the M4 forecasting competition of Makridakis et al. (2018). In order to reduce the computation volume related to the extensive backtests, we use $N = 100$ data sets of each $n = 20$ daily, weekly, monthly, quarterly and yearly data while the number of elements is limited to $n_d = 1000$ daily, $n_w = 500$ weekly, $n_m = 250$ monthly, $n_q = 100$ quarterly and $n_y = 75$ yearly data points. For a complete list of variables see Table 1 in the Appendix.

To test the quality of the synthetic data generated by the different augmentation methods, we conduct a series of experiments. The first three experiments test for the similarity of synthetic and real instances via different approaches. The first test uses a dimensionality reduction technique to visualize synthetic and real data sequences. The second test trains a recurrent neural network on synthetic data to predict real data while the third test trains a classifier to distinguish between real and synthetic sequences. A final fourth test evaluates the benefit of the augmentation methods by training a model on varying levels of generated data.

The first test applies the the Uniform Manifold Approximation and Projection (UMAP) algorithm (McInnes et al., 2020) for clustering. A similar approach has been applied by Yoon et al. (2019); Ali et al. (2019) and treats each of the d time steps as an individual feature. The UMAP algorithm receives sequences of length $D_{seq} = 28$ and reduces the dimension to $D_{umap} = 2$. Elements located closely in the 2D space are likely to have similar characteristics. Then, we plot the representation in $d = 2$ and randomly choose up to $n = 500$ synthetic and real sequences, depending on the size of the initial data set. The individual points are colored to indicate which are original or synthetic. In case, real and synthetic time series are clearly different, we observe two distinct clusters with small distance inside each cluster and a large difference to the other cluster(s). Else, we observe one or more mixed clusters with heterogeneous distribution of real and synthetic elements inside each cluster. Figure 1 (a) contains the clustering result of a weekly data set (W77).

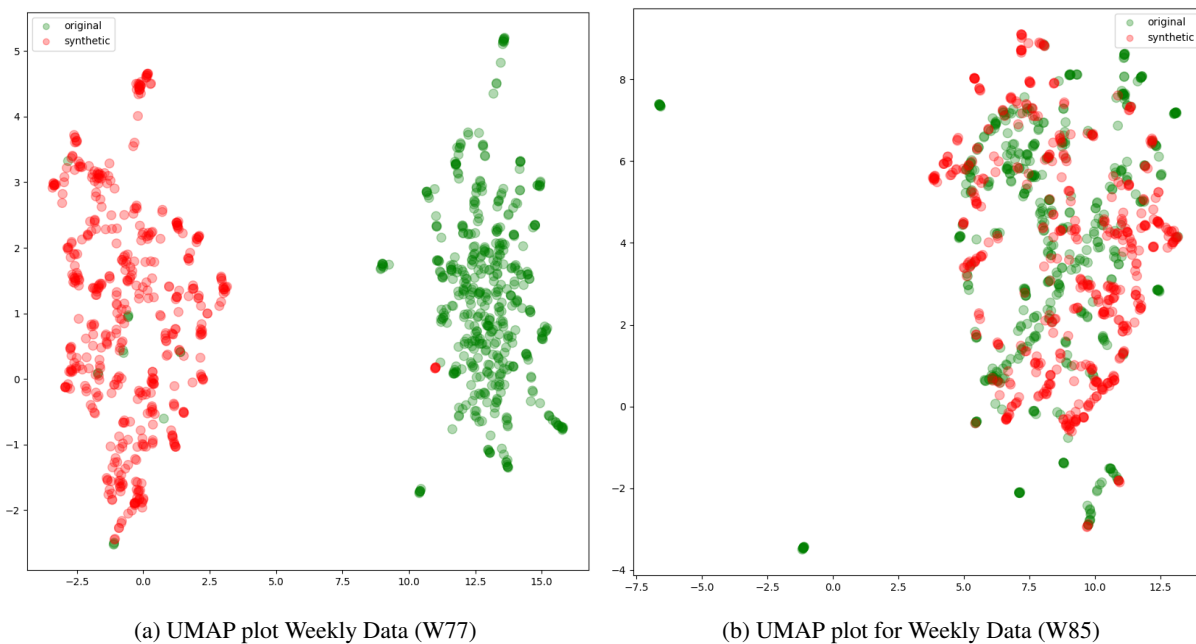


Figure 1: Selected UMAP Results

The original data (green) and the generated data (red) separate with few exceptions in two distinguishable clusters indicating deficient sample quality. Here, the samples are significantly different such that the UMAP algorithm can easily differentiate between them. An increased homogeneity in the samples is displayed Figure 1 (b). It shows real and synthetic instances of weekly data (W85), but displays a single large cluster mixed with synthetic and real instances. Except for a few outliers, synthetic and real elements mix well, while the synthetic instances have a slightly more wide-spread cluster. This is an example of a successful augmentation where the UMAP algorithm cannot distinguish between original and synthetic elements. Due to the high number of data sets we only show two exemplary UMAP plots at this point.

After a first qualitative assessment, the next test performs a predictive assessment on the synthetic data. In order to get more detailed information whether the augmentation is useful for predicting the real data, we train a recurrent neural network (RNN) solely on synthetic instances before predicting the real instances. We choose a small LSTM network of $n_{hl} = 3$ hidden layers with $n_{ne} = 7$ neurons each. In case the augmentation method works well, a model trained on

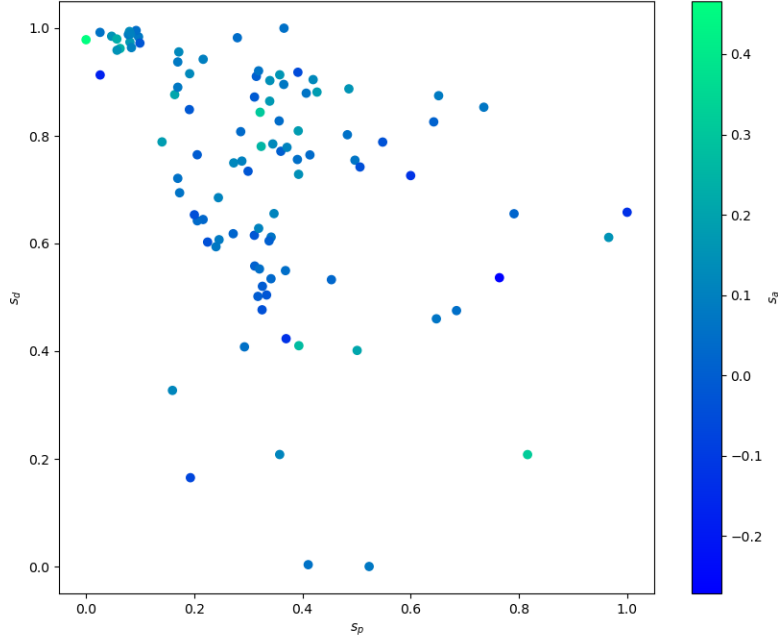


Figure 2: Relation between Predictive, Discriminative and Augmentation Score

synthetic data predicts real data accurately. To assess the quality we perform a 80/20 split for train and test set. The training process is repeated $k = 10$ times and uses early stopping after $c = 5$ periods on the mean absolute error of the test set to counter imperfect initialization and overfitting. The predictive score s_p for all data sets can be obtained from Table 1 in the Appendix section.

The third, discriminative test, acts a quantitative expansion to the first qualitative test and assesses whether a generated time series is reasonably similar to the original time series. Again, a RNN is trained on sequences of length $D = 28$ but now with the goal to distinguish real and synthetic instances with the same split for train and test data as well as early stopping on the binary crossentropy error. Again, we choose a small LSTM network with $n_{hl} = 3$ hidden layers with $n_{ne} = 8$ neurons each. The discriminative score s_d can be obtained from Table 1 in the Appendix section.

A fourth experiment examines the augmentation benefit for the WGAN-GP trained on the XIRPs for each of the data sets. Therefore an RNN is trained stepwise with an increasing fraction of synthetic data ranging from 0% to 50%. At each step a train/test split shuffles the sequences and randomly assigns them to one of the sets. The RNN is evaluated analogously to the predictive test using the same early stopping mechanism. Note, that the test and validation set always consist of real data instances to keep synthetic elements in the training set and thus avoid corrupting reliability of the performance measure. A train/test split of 80/20 is kept throughout the test. For each fraction of synthetic data α we repeat the test $k = 10$ times to improve the stability of the results. As a reference, we choose $RMSE_{\alpha=0}$ and then use the percentage improvement compared to the optimal level $RMSE_{\alpha^*}$. Figure 2 plots the three scores s_p , s_d and s_a and their relationship.

In case of perfect alignment, we could observe a clear relationship, be it linear, quadratic or cubic and see a gradular color change along either axis. A look at the relationships between the scores via the Spearman rank correlation coefficient ρ_r displayed in Table 2 supports the impression of the plot, that there is a negative relationship between s_d and s_p , namely $\rho_r(s_d, s_p) = -0.4469$. The negative sign originates from the construction of the scores, since a small predictive, high discriminative and high augmentation scores are optimal. The relationship of the augmentation benefit towards predictive and discriminative score is less distinct. Its interaction with the predictive score $\rho_r(s_a, s_p) = -0.1359$ is a slightly negative one, while $\rho_r(s_a, s_d) = 0.2837$ is slightly positive. Since the measures account for different aspects of the generative model, they are designed to be slightly correlated but not perfectly aligned, which would indicate redundancy.

An important aspect when augmenting data, is to what extent we can reduce the forecast error. In a first approach, inspect the augmentation score in terms of percentage decrease in RMSE on the frequency domain. The scores

ρ	s_a	s_p	s_d
s_a	1	-0.1359	0.2837
s_p	0.1359	1	0.4469
s_d	-0.2837	-0.4469	1

Table 1: Spearman rank correlation between the test scores

aggregated over all frequencies and plotted in Figure 3 (a) shows that some data sets benefit from augmentation resulting in a decrease the error by 30% while for other data sets, augmentation is not successful resulting in larger forecasting errors and thus a negative s_a . On average, the RMSE decreases by $\mu = 0.07$ or 7%. Taking a closer look at the daily data in Figure 3(b) shows that for a daily frequency the benefit diverges to either small positive/negative benefits or large benefits. For weekly data μ stays roughly unchanged and the data almost resembles a uniform distribution from $s_a = -0.05$ to $s_a = 0.15$. For monthly data $\mu = 0.04$ is smaller but differs little regarding the variance. Regarding the quarterly and yearly data in Figures 3(e) and 3(f) we see a slight shift in the mean towards a higher augmentation benefit.

In all six frequencies we see only little differences in terms of μ , which is surprising, since the observations and their data generating process are different in nature. Nevertheless, the WGAN-GP approach with XIRPs is able to improve 85% of the daily data, 75% of the weekly, 70% of the monthly, 90% of the quarterly data and 75% of the yearly data sets.

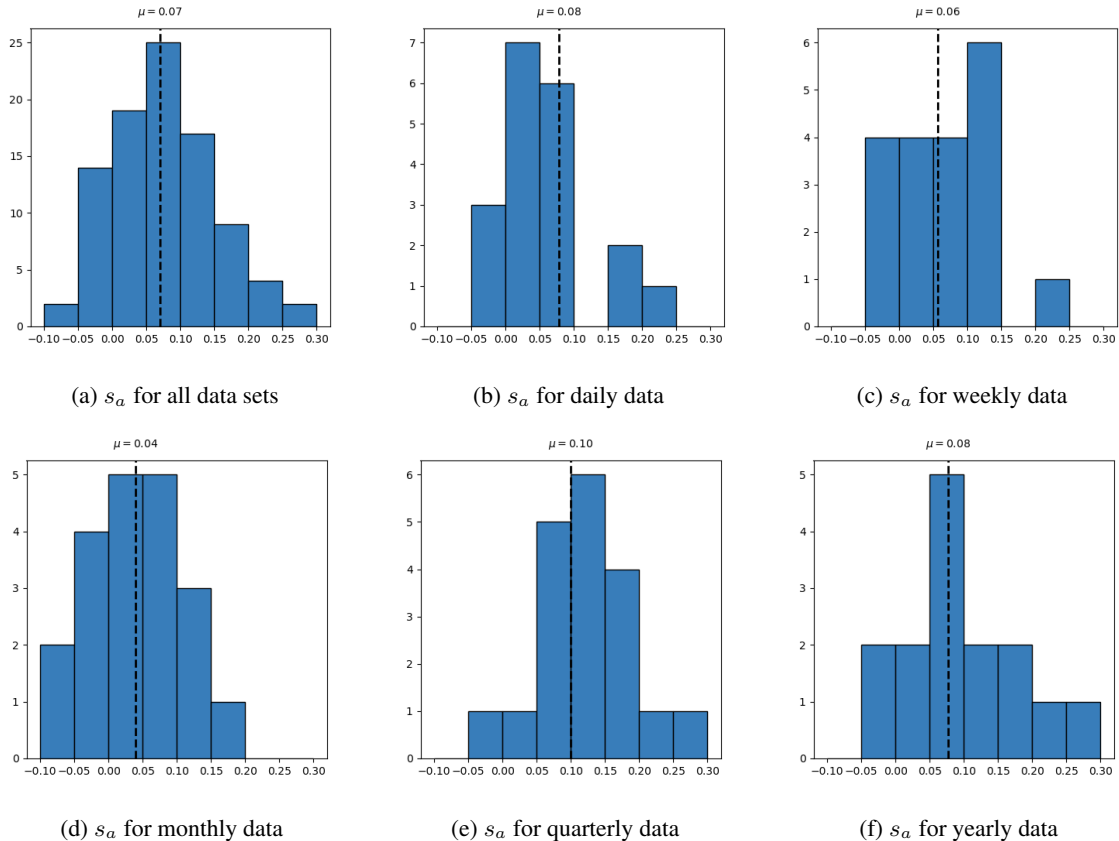


Figure 3: Augmentation Score Distribution

In the following step, we explore the optimal amount of augmented data α_* and therefore consider the distribution of α . The results are displayed in Figure 4 where we see relatively huge bars for $\alpha = 0$, which corresponds to an unsuccessful augmentation. In this case the best is to omit generated data. The results look similar for all frequencies with varying μ except of the quarterly data. The α_* for quarterly data exhibits a large proportion of high augmentation levels, where 5

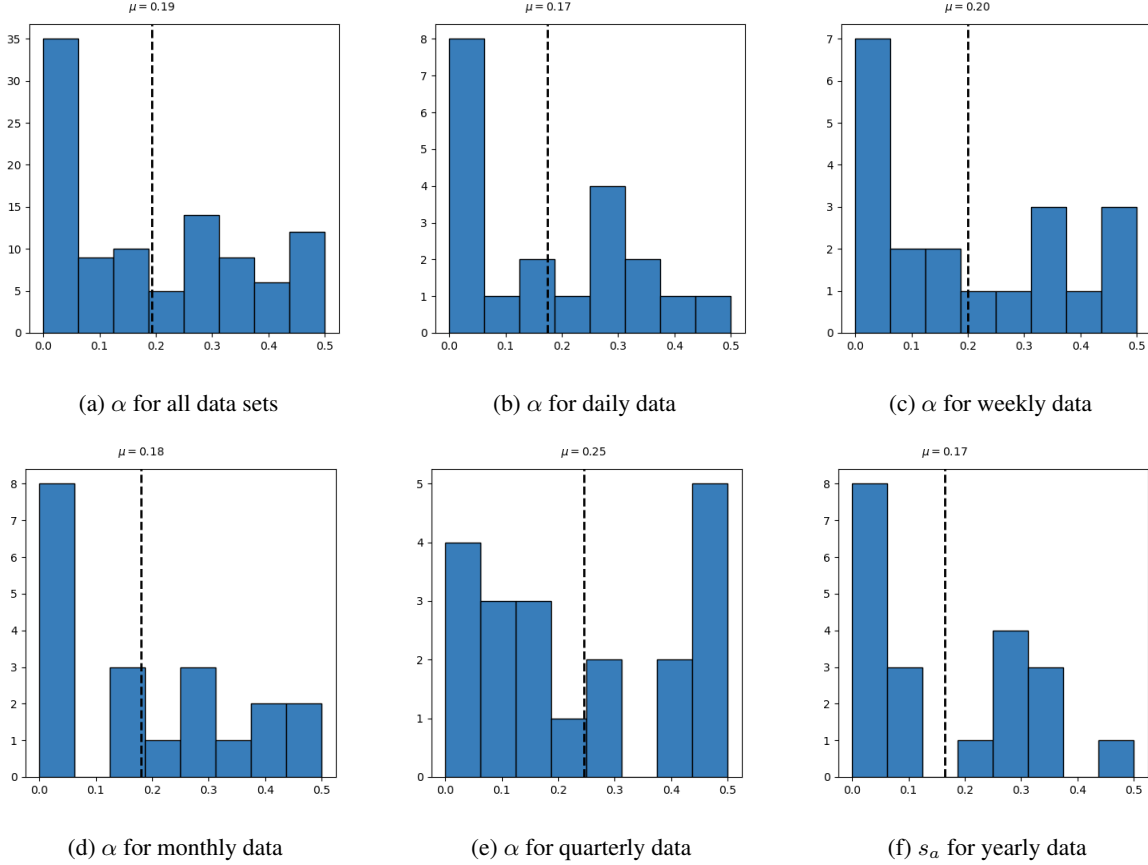


Figure 4: Augmentation Level Distribution

out of 20 data sets can be augmented up to a rate of 50% of generated data. This is interesting since compared to the next lower frequency of yearly data, this is only the case for 1 in 20 data sets. Over all financial data sets, we can see that on average $\alpha_* = .2$ or a level of roughly 20% of generated data lowers the forecast error in the most effective way. In Figures 3 and 4 we can see that s_α and α_* vary in and across the different frequencies. In order to know, which factors drive not only s_a but also s_p and s_d , we apply the concept of Shapley values to a set of moments (mean μ , variance, σ^2 , skewness μ_3 and kurtosis μ_4) contained in Table 1 as well as the results from the previous discriminative and predictive tests. Besides the descriptive statistics, we add the value of Ljung-Box test statistic to quantify whether a group of autocorrelations differ from zero Ljung and Box (1978); Box and Pierce (1970). With H_0 the test assumes the data is independently distributed and thus any correlations must be of random nature. The number of lags being tested over is denoted by h and we can reject H_0 if the test statistic¹ $Q > \chi^2_{1-\alpha, h}$. To incorporate the commonly present behavior of volatility clustering, the test is conducted once on the raw returns Q_r and on the absolute returns $Q_{|r|}$ to capture large sequential movements with both signs.

In order to make a statement on the influence of features regarding the output, we regress the calculated statistics sequentially on s_p , s_d , s_a and α^* . We train a neural network regression model with $n_{hl} = 2$ hidden layers of $n_{ne} = 10$ neurons each and use early stopping as regularization. Figure 5 shows the Shapley values for the different characteristics of the data set where each represented by a dot. The corresponding plots sort the features regarding their importance from top to bottom and plot the Shapley value of each instance against its feature value indicated by the coloring from blue (low) to cyan (high). In Figure 5(a) we can see that the high first order autocorrelation of returns, denoted by Q_r , leads to a smaller s_p . Please remind at this point, that the smaller s_p , the better the generated data. This appears reasonable, since highly correlated time series are easier to predict than time series with little autocorrelation. For Q_r multiple dots with high feature values (cyan) are visible. For the variance we see an opposite behavior, of high variance leading to a higher and thus worse predictive score. In addition, datasets with higher μ_4 and μ result in a higher s_p , while μ_3 has the tendency to improve s_p . What we can see here is that the features mainly have either small positive or

¹The test statistic is calculated via $Q = n(n+2) \sum_{k=1}^h \frac{\hat{\rho}_k^2}{n-k}$ with sample size n and sample autocorrelation $\hat{\rho}$ at lag k

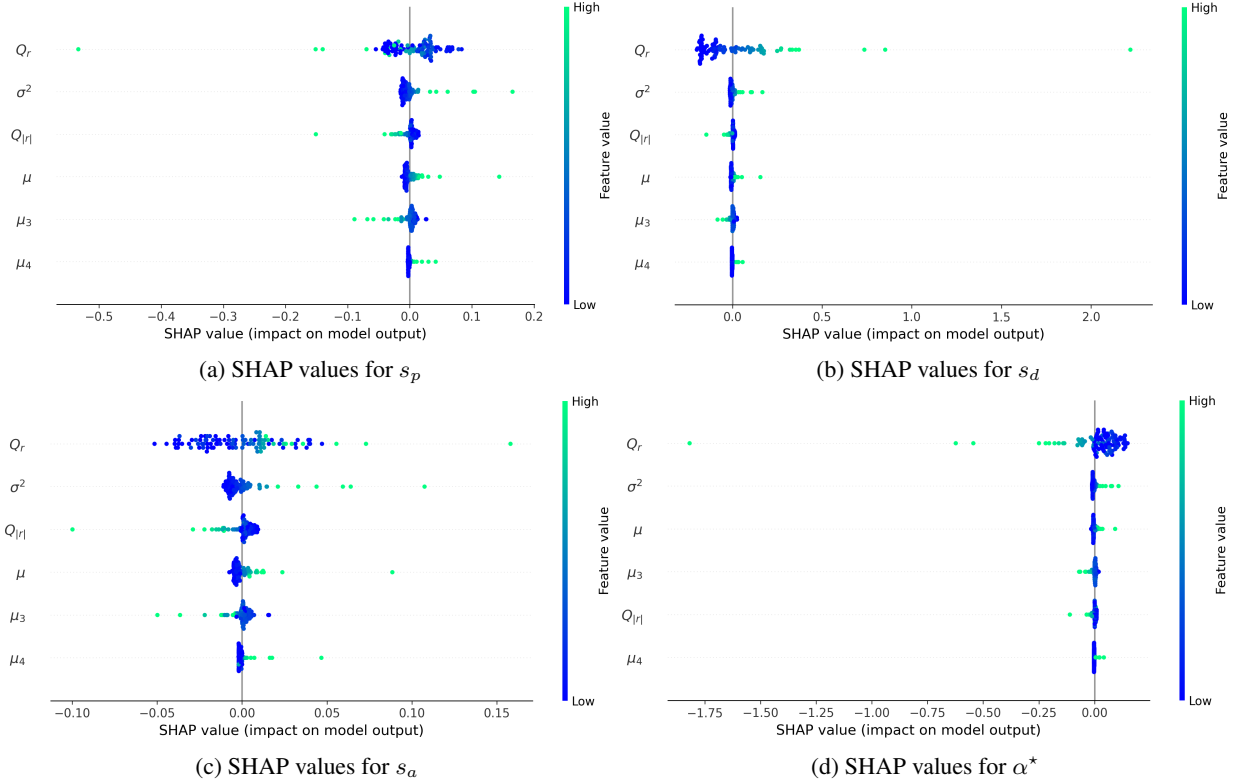


Figure 5: Shapley Values for s_p , s_d , s_a and α^*

small negative effect and contribute largely only in case of extreme feature values. For the discriminative score in Figure 5(b), we observe the same order in the feature importance. Interestingly, only the results of Q_r reverse their effects, since one would expect the opposite effects consistently for all variables. But as mentioned above, the discriminative score measures a different aspect of the generation process. For the discriminative score, a higher variance leads to a higher discriminative score, which is reasonable, since a data set with $\sigma^2 = 0$ would be easily distinguishable from generated data, which naturally comes with some variance.

The Shapley value for the augmentation benefit s_a are of particular interest for this paper. For Q_r we can observe multiple interesting effects. The plot proposes that an average feature value increases the augmentation score. On the one hand, instances with a medium low level of Q_r seem to improve the score. On the other hand elements with very low and very high feature values both increase the benefit of augmentation. Regarding s_a , this behavior is not observed for any other feature. Strikingly, compared to Q_r , opposite effects can be observed for $Q_{|r|}$. It has the opposing effect not only in Figure 5(c) but also in the previous ones. Return distributions with high μ_3 seem to harm s_a while excess μ_4 improves the augmentation benefit. However, the second and third moment are of relatively small importance compared to Q_r and σ , unless they have high feature values.

Regarding the choice of α^* , we see in Figure 5(d) that smaller values of Q_r have a small positive influence, but the higher values the more they reduce α^* . This means for data sets with high autocorrelation there exists the tendency to reduce the optimal level of α^* . The opposite applies for σ^2 and μ which have the tendency to favor higher fractions of generated data for higher features. It is clearly observable that all features except Q_r have little effect on α^* unless they take high values. Throughout the evaluation of s_p , s_d , s_a , α^* we see that the test statistic of the Ljung Box test provides most information regarding the Shapley values. The other features become only relevant once their values are high. However, we cannot make a deterministic statement which level of α is the best, but we can surely provide some guidance on whether an augmentation is likely to be successful and limit the search space for an exhaustive search of α .

5 Conclusion

This paper evaluates the image-based financial time series augmentation method for the first time. The new extended IRP encodes the initial time series as well as its intertemporal dynamics in a single image. In a sequence of tests the data augmentation increases the performance of return forecasting models substantially. This is valid for all considered data frequencies (daily, weekly, monthly, quarterly and yearly) where the model decreased the average forecasting error by 7%. In a series of tests and multiple repetitions we observe an optimal amount of augmented data ranging from 17-25% and the forecast error was reduced by 79% of the datasets. Further, Shapley values identify important features such as low variance and high autocorrelation to have positive effects on the quality of the simulated returns indicated by the performance metrics. In addition, the distribution of optimal augmentation levels proposes a fraction of 19% of synthetic data over all data frequencies. In a more far reaching study, the number of predictors in the analysis could be extended to account for drifts, seasonality and jump frequency. Further, a cross model comparison with other time series augmentation methods could provide useful benchmarks regarding the efficiency of the WGAN-GP trained on XIRP.

6 Appendix

Table 2: Data Sets and Characteristics

	Q_r	$Q_{ r }$	μ	σ^2	μ_3	μ_4	s_p	$\sigma(s_p)$	s_d	$\sigma(s_d)$
D2036	12.6789	111.7431	0.0002	0.005	3.7249	43.3613	0.062	0.0017	0.6652	0.0017
D2037	0.555	21.0601	-0.0001	0.0084	0.5399	2.0599	0.2975	0.0169	0.5348	0.0169
D2041	11.0322	23.4504	0.0002	0.0098	-0.0527	5.139	0.1836	0.007	0.4483	0.007
D2042	0.3416	0.1499	0.0024	0.0649	30.2191	938.9764	0.0121	0.0028	0.6763	0.0028
D2044	0.1183	59.4217	0.0003	0.0283	0.6016	3.211	0.2592	0.0137	0.3893	0.0137
D2045	0.0339	7.5565	-0.0002	0.011	0.2256	0.329	0.3716	0.0231	0.372	0.0231
D2046	35.2578	30.4177	-0.0	0.019	0.0447	6.9086	0.1751	0.007	0.4467	0.007
D2047	1.8137	36.0486	-0.0003	0.0075	-0.7468	5.4485	0.207	0.006	0.4227	0.006
D2079	10.8896	20.7505	0.0003	0.0087	-0.0432	3.5599	0.2495	0.0095	0.5095	0.0095
D2081	0.8412	73.8237	-0.0	0.0092	0.0222	9.1041	0.1708	0.0038	0.4543	0.0038
D2082	0.0357	119.6404	-0.0004	0.0105	-0.3877	9.7545	0.1492	0.0031	0.4822	0.0031
D2100	0.0863	0.6849	0.0	0.0079	-6.7288	85.8972	0.089	0.0125	0.6799	0.0125
D2116	2.2632	5.8627	0.0001	0.0073	-2.9239	61.3999	0.0764	0.0035	0.6733	0.0035
D2120	2.6408	1.1318	-0.0001	0.0133	12.3916	196.2792	0.0496	0.0023	0.6807	0.0023
D2138	0.2903	113.5562	0.0001	0.0193	-1.6667	26.1115	0.0786	0.0042	0.6663	0.0042
D2194	0.8931	1.4466	0.0001	0.0036	-7.5221	115.8853	0.0741	0.0102	0.6829	0.0102
D2215	1.7563	0.3823	0.0001	0.0078	-6.6697	84.9711	0.091	0.0043	0.672	0.0043
D2229	13.3545	58.4232	0.0007	0.0175	0.0798	7.4643	0.2277	0.0101	0.4303	0.0101
D2230	5.8682	6.7573	0.0003	0.0145	3.9521	59.8002	0.0855	0.0057	0.688	0.0057
D2231	0.0697	5.2598	0.0009	0.0288	16.5995	449.2814	0.0326	0.0055	0.6856	0.0055
W60	35.874	42.4429	0.0002	0.007	-0.4752	7.7464	0.206	0.0124	0.476	0.0124
W61	0.0015	107.3888	0.0019	0.0451	-0.275	3.7143	0.2705	0.0173	0.3636	0.0173
W62	47.6821	0.1146	0.0039	0.0593	0.4979	4.0707	0.1465	0.0081	0.616	0.0081
W63	53.517	1.516	0.0033	0.0549	-0.1422	0.0915	0.2803	0.0279	0.4212	0.0279
W64	0.0533	0.3811	0.0004	0.0207	0.2717	0.2117	0.2639	0.0139	0.3508	0.0139
W65	0.0657	2.5205	0.0013	0.02	0.3341	-0.0684	0.27	0.0176	0.3338	0.0176
W66	291.3217	283.761	0.0021	0.0114	6.8511	63.1087	0.0572	0.0029	0.6772	0.0029
W67	56.1576	36.7007	0.0015	0.0058	-0.4601	4.8849	0.1837	0.0118	0.6515	0.0118
W68	1.6342	6.3722	0.0046	0.0129	1.6228	12.5211	0.148	0.0114	0.6608	0.0114
W69	16.1796	5.3771	0.003	0.0104	-0.3818	5.4845	0.1465	0.0113	0.6481	0.0113

Continued on next page

Table 2: Data Sets and Characteristics (Continued)

Q_r	$Q_{ r }$	μ	σ^2	μ_3	μ_4	s_p	$\sigma(s_p)$	s_d	$\sigma(s_d)$
W74	31.1916	0.0048	0.0576	1.6475	11.4199	0.1639	0.0061	0.6332	0.0061
W75	20.2453	0.005	0.0691	1.6976	11.8365	0.1635	0.0046	0.5877	0.0046
W77	7.5487	0.03	0.4365	16.8983	336.1388	0.0328	0.0054	0.6316	0.0054
W78	0.9187	0.0402	0.4152	9.7178	137.2073	0.0575	0.009	0.663	0.009
W79	49.1523	-0.001	0.0506	-0.0359	0.7106	0.3043	0.017	0.3835	0.017
W80	13.4888	-0.0006	0.0565	-0.0163	1.0408	0.2831	0.0109	0.3732	0.0109
W81	2.9919	0.0046	0.0541	0.7962	4.3767	0.2387	0.0172	0.5597	0.0172
W82	9.3028	0.0014	0.0101	-1.1435	8.9698	0.1465	0.0079	0.5005	0.0079
W85	118.4298	0.0043	0.0155	-3.8171	36.1468	0.0757	0.0087	0.6867	0.0087
W86	59.4326	0.0043	0.0168	-3.7042	33.2741	0.0772	0.0109	0.6836	0.0109
M36737	29.2602	-0.0012	0.0274	0.2258	0.3024	0.3225	0.0165	0.635	0.0165
M36738	34.4594	0.003	0.0244	0.5146	1.0417	0.395	0.0111	0.5558	0.0111
M36739	28.1722	-0.0037	0.027	-0.4383	0.7614	0.3401	0.0166	0.5302	0.0166
M36740	37.2228	-0.0005	0.013	0.568	5.1133	0.175	0.0077	0.5304	0.0077
M36741	14.4481	0.0035	0.0296	3.5729	26.7611	0.165	0.0277	0.1209	0.0277
M36742	26.7934	-0.0005	0.0176	-0.0221	0.1303	0.295	0.0201	0.5733	0.0201
M36743	25.4588	-0.001	0.0218	0.1326	0.357	0.3347	0.0164	0.6085	0.0164
M36744	21.8721	-0.0007	0.0179	0.0255	0.1183	0.3218	0.0229	0.5244	0.0229
M36745	0.3586	0.0018	0.0883	1.1682	10.5803	0.2442	0.0101	0.2868	0.0101
M36746	0.3389	0.0069	0.0345	-0.4902	1.4241	0.2766	0.0171	0.3526	0.0171
M36747	5.3149	0.0016	0.0081	-1.0771	1.4126	0.2833	0.0202	0.426	0.0202
M36748	7.157	0.0035	0.0188	-0.7633	0.3945	0.2662	0.0189	0.3856	0.0189
M36749	0.0963	0.0044	0.0082	-0.5915	0.5769	0.2587	0.0293	0.4283	0.0293
M36750	3.8707	0.0073	0.0055	-0.7902	0.7094	0.2404	0.0104	0.5224	0.0104
M36751	105.8418	0.0092	0.0072	0.0599	1.0761	0.2616	0.0132	0.6298	0.0132
M36752	61.0842	0.0099	0.0477	10.9394	142.6069	0.1387	0.0181	0.2316	0.0181
M36753	0.0121	0.0034	0.0334	0.3755	4.4235	0.1902	0.0145	0.4197	0.0145
M36754	13.197	0.0134	0.0982	0.6236	8.4962	0.1234	0.0092	0.5467	0.0092
M36755	0.0355	0.0037	0.0171	-0.2838	0.7437	0.2857	0.0156	0.5441	0.0156
M36757	2.6373	0.0047	0.0346	-1.2927	7.2291	0.2025	0.0105	0.4138	0.0105

Continued on next page

Table 2: Data Sets and Characteristics (Continued)

Q_r	$Q_{ r }$	μ	σ^2	μ_3	μ_4	s_p	$\sigma(s_p)$	s_d	$\sigma(s_d)$	
Q17832	8.4037	0.0149	0.0004	0.0232	-0.4884	0.5335	0.3448	0.0075	0.6257	0.0075
Q17833	16.1497	4.1563	0.0156	0.0176	-1.08	3.0366	0.2285	0.0168	0.5201	0.0168
Q17834	3.4132	5.7612	0.0293	0.0231	0.7119	1.2563	0.3065	0.0162	0.5398	0.0162
Q17835	0.2641	0.0443	-0.0045	0.0246	-0.6486	1.3741	0.2814	0.0063	0.6245	0.0063
Q17836	0.3292	0.3008	0.0219	0.0275	0.5822	1.8323	0.3018	0.0066	0.6196	0.0066
Q17837	0.0015	0.0992	0.0321	0.1004	6.475	53.4929	0.4269	0.0506	0.0083	0.0506
Q17838	0.2867	0.1703	0.0288	0.0485	1.4792	4.5525	0.2687	0.0324	0.541	0.0324
Q17839	0.1647	1.6294	0.0341	0.0282	0.4536	0.2891	0.3505	0.0289	0.6099	0.0289
Q17840	13.8117	0.204	0.2617	0.6295	-0.6139	-0.9383	0.6178	0.0283	0.3745	0.0283
Q17841	0.0044	3.2708	0.0033	0.0525	0.2618	-1.1696	0.5254	0.0407	0.3224	0.0407
Q17842	23.7412	9.1132	0.0038	0.033	0.8002	1.1311	0.3235	0.03	0.5056	0.03
Q17843	27.3681	13.7544	0.0148	0.0163	-0.7502	1.8423	0.2589	0.0133	0.6036	0.0133
Q17844	0.002	0.6447	-0.0057	0.0268	-0.4359	1.355	0.2649	0.0164	0.6368	0.0164
Q17845	10.6369	4.8357	0.0098	0.1609	0.2143	4.0562	0.2812	0.0171	0.5984	0.0171
Q17846	0.1361	0.293	0.032	0.0993	3.9938	27.7409	0.3376	0.0023	0.0106	0.0023
Q17847	7.562	0.4206	0.0073	0.0173	-0.9662	2.5303	0.323	0.0274	0.5607	0.0274
Q17848	33.8833	20.9188	0.0179	0.0198	-0.6399	1.5836	0.2338	0.011	0.6788	0.011
Q17849	26.9451	9.5063	0.0243	0.0277	0.8078	2.2681	0.2875	0.0189	0.4558	0.0189
Q17850	2.9854	3.0398	0.0188	0.0199	0.5516	1.3983	0.2959	0.0204	0.6318	0.0204
Q17851	2.4744	0.7059	0.0014	0.0212	1.2099	14.3911	0.142	0.0134	0.6067	0.0134
Y15255	17.3125	12.2725	0.0373	0.0508	-0.5322	2.3565	0.7779	0.0591	0.4256	0.0591
Y15256	17.6607	11.3819	0.0384	0.0554	-0.4008	2.3202	0.5949	0.0725	0.5907	0.0725
Y15264	16.4772	13.3423	0.0243	0.0733	0.3084	2.6039	0.4877	0.0003	0.504	0.0003
Y15275	36.5599	32.0065	0.0244	0.049	0.2569	2.5199	0.5287	0.0494	0.6053	0.0494
Y15276	34.3218	24.5217	0.025	0.0474	-0.2765	2.9901	0.8049	0.0782	0.4575	0.0782
Y15277	32.6989	18.3289	0.0074	0.0436	0.3294	1.7396	0.4061	0.0178	0.5235	0.0178
Y15279	21.226	11.3308	0.0242	0.0674	0.3749	2.028	0.3021	0.0096	0.6909	0.0096
Y15281	7.6237	4.6061	0.0188	0.0538	0.0352	3.1612	0.6392	0.053	0.4556	0.053
Y15285	18.3394	9.5559	0.019	0.0544	1.5419	4.7511	0.3972	0.0091	0.614	0.0091
Y15286	12.5469	4.4191	0.0193	0.0278	0.6707	1.1706	0.5215	0.0406	0.5721	0.0406

Continued on next page

Table 2: Data Sets and Characteristics (Continued)

Q_r	$Q_{ r }$	μ	σ^2	μ_3	μ_4	s_p	$\sigma(s_p)$	s_d	$\sigma(s_d)$	
Y15292	26.3967	24.2216	0.0291	0.0371	-1.2502	4.2043	0.5549	0.0477	0.3328	0.0477
Y15835	3.3513	4.2464	0.0207	0.0274	0.0771	-0.1142	0.4467	0.0351	0.5465	0.0351
Y15836	4.6649	15.1757	0.002	0.0396	-1.8682	9.1205	0.3239	0.0449	0.2883	0.0449
Y15837	0.0002	0.4006	0.0004	0.0333	-0.3175	4.0875	0.2671	0.0285	0.5843	0.0285
Y15838	0.0002	2.1539	0.0057	0.0843	1.0592	4.6235	0.4135	0.0575	0.5149	0.0575
Y17075	0.3335	0.2484	0.006	0.0625	-4.9327	34.6798	0.659	0.0719	0.1502	0.0719
Y17124	0.5078	4.8133	0.0717	0.22	1.2986	12.1372	0.265	0.0546	0.4371	0.0546
Y17232	6.3279	11.4126	0.095	0.4226	1.5396	4.8984	0.2958	0.0422	0.1503	0.0422
Y17248	18.4507	18.5384	0.0495	0.0506	1.7588	3.8869	0.3052	0.0272	0.2972	0.0272
Y17249	45.5972	39.0945	0.0492	0.0654	0.7146	-0.5938	0.4093	0.0616	0.2823	0.0616

Table 2: Augmentation Benefit for Multiple Levels of Generated Data α

	$\alpha = 0$	$\alpha = 0.05$	$\alpha = 0.1$	$\alpha = 0.15$	$\alpha = 0.2$	$\alpha = 0.25$	$\alpha = 0.3$	$\alpha = 0.35$	$\alpha = 0.4$	$\alpha = 0.45$	$\alpha = 0.5$	α^*
D2036	0.1068	0.0956	0.1024	0.0813	0.0963	0.0892	0.0971	0.0916	0.0961	0.0879	0.0901	0.15
D2037	0.2136	0.2126	0.2139	0.2208	0.2248	0.2271	0.2329	0.2383	0.2378	0.2379	0.2418	0.05
D2041	0.1604	0.1591	0.1591	0.1659	0.1562	0.1702	0.1668	0.1636	0.1637	0.1678	0.1653	0.2
D2042	0.0526	0.0334	0.0548	0.0496	0.0653	0.0281	0.052	0.0351	0.0435	0.0634	0.0541	0.25
D2044	0.2256	0.2233	0.2294	0.231	0.2274	0.2337	0.2381	0.2352	0.2305	0.2452	0.242	0.05
D2045	0.2773	0.2703	0.2791	0.2775	0.2865	0.2859	0.2865	0.2995	0.2875	0.2903	0.29	0.05
D2046	0.169	0.1676	0.1682	0.1627	0.1741	0.1642	0.1729	0.1723	0.171	0.1788	0.1727	0.15
D2047	0.2015	0.1856	0.1851	0.1912	0.194	0.1929	0.1906	0.2001	0.185	0.192	0.1902	0.4
D2079	0.199	0.2093	0.2097	0.2048	0.2032	0.2048	0.2062	0.2032	0.2049	0.2047	0.2047	0.0
D2081	0.1411	0.1497	0.1525	0.1514	0.1541	0.1472	0.151	0.1488	0.1477	0.1516	0.1525	0.0
D2082	0.1444	0.1358	0.1409	0.1411	0.1375	0.1356	0.1434	0.1387	0.147	0.1464	0.1436	0.25
D2100	0.1234	0.1165	0.1213	0.135	0.118	0.1139	0.1293	0.115	0.1186	0.1296	0.1313	0.25
D2116	0.1038	0.105	0.0967	0.0963	0.0866	0.0974	0.0863	0.0976	0.093	0.0868	0.0947	0.3
D2120	0.0993	0.1234	0.122	0.1	0.097	0.1089	0.1183	0.0841	0.1333	0.1051	0.1063	0.35
D2138	0.1153	0.1209	0.1119	0.1128	0.1161	0.1198	0.1168	0.1107	0.1173	0.1201	0.1039	0.5
D2194	0.0832	0.0772	0.0966	0.0871	0.0901	0.11	0.0948	0.0941	0.1013	0.0983	0.097	0.05
D2215	0.1543	0.1583	0.1682	0.1577	0.1611	0.1629	0.168	0.1655	0.1698	0.1719	0.1914	0.0
D2229	0.2148	0.2171	0.2138	0.2123	0.2263	0.2139	0.2173	0.2105	0.2185	0.2149	0.2231	0.35
D2230	0.1007	0.1049	0.0958	0.1	0.1223	0.1082	0.0975	0.1027	0.1045	0.0973	0.1112	0.1
D2231	0.0345	0.0325	0.0708	0.0662	0.0503	0.0689	0.054	0.0491	0.0607	0.0474	0.0533	0.05
M36737	0.3309	0.3686	0.3682	0.3566	0.3532	0.3596	0.367	0.3486	0.3721	0.3548	0.3536	0.0
M36738	0.3275	0.3339	0.3331	0.3313	0.3229	0.3425	0.329	0.3089	0.3426	0.3557	0.3667	0.35
M36739	0.354	0.3491	0.3457	0.3653	0.3481	0.3527	0.3476	0.3629	0.3423	0.341	0.3526	0.45
M36740	0.2053	0.2254	0.2175	0.2314	0.246	0.2136	0.2367	0.2094	0.2305	0.2315	0.2064	0.0
M36741	0.145	0.1726	0.1586	0.1549	0.1603	0.1855	0.1616	0.1825	0.1748	0.1759	0.1592	0.0
M36742	0.3327	0.3306	0.3331	0.3415	0.3483	0.3187	0.3458	0.3227	0.341	0.343	0.3411	0.25
M36743	0.3497	0.3368	0.3533	0.353	0.3403	0.3484	0.3336	0.3396	0.3277	0.327	0.3361	0.45
M36744	0.3464	0.3461	0.3314	0.3502	0.3461	0.3434	0.3411	0.3537	0.3291	0.3411	0.3432	0.4
M36745	0.1888	0.2178	0.1997	0.1787	0.2107	0.193	0.2106	0.1848	0.2132	0.2124	0.185	0.15
M36746	0.151	0.1638	0.1548	0.1698	0.1656	0.1614	0.1793	0.1808	0.1873	0.1965	0.1821	0.0
M36747	0.1878	0.176	0.2302	0.2286	0.194	0.216	0.2122	0.2148	0.2346	0.2441	0.2061	0.05
M36748	0.1516	0.1719	0.1579	0.1444	0.1564	0.1904	0.1634	0.1795	0.1781	0.173	0.1753	0.15

Continued on next page

Table 2: Augmentation Benefit for Multiple Levels of Generated Data α (Continued)

	$\alpha = 0$	$\alpha = 0.05$	$\alpha = 0.1$	$\alpha = 0.15$	$\alpha = 0.2$	$\alpha = 0.25$	$\alpha = 0.3$	$\alpha = 0.35$	$\alpha = 0.4$	$\alpha = 0.45$	$\alpha = 0.5$	α^*
M36749	0.1768	0.1808	0.1859	0.2032	0.2021	0.2005	0.223	0.2079	0.2298	0.2151	0.2355	0.0
M36750	0.2338	0.2283	0.2361	0.2343	0.2101	0.2256	0.2274	0.2275	0.2185	0.2259	0.2486	0.2
M36751	0.2583	0.2774	0.2603	0.2731	0.2658	0.2679	0.2574	0.279	0.2917	0.2703	0.284	0.3
M36752	0.092	0.0875	0.093	0.1111	0.1647	0.1342	0.1213	0.0869	0.0813	0.1532	0.1361	0.4
M36753	0.2035	0.2113	0.2272	0.2172	0.2304	0.2398	0.234	0.2241	0.2265	0.2384	0.2302	0.0
M36754	0.189	0.1942	0.1706	0.1955	0.178	0.1548	0.2003	0.1807	0.1939	0.1817	0.1886	0.25
M36755	0.3216	0.2829	0.3116	0.3208	0.3192	0.3263	0.3229	0.3257	0.3249	0.3236	0.3363	0.05
M36757	0.2244	0.2296	0.2226	0.2081	0.2402	0.2221	0.2085	0.2213	0.2098	0.2136	0.2237	0.15
Q17832	0.4405	0.4378	0.3868	0.4255	0.4062	0.4228	0.4041	0.4184	0.4174	0.4068	0.4047	0.1
Q17833	0.2885	0.2542	0.3	0.3194	0.2754	0.2799	0.3096	0.292	0.2889	0.272	0.2954	0.05
Q17834	0.3943	0.3896	0.3835	0.3709	0.3971	0.4388	0.3522	0.4004	0.4052	0.4108	0.3626	0.3
Q17835	0.3846	0.3678	0.3289	0.3296	0.3635	0.3783	0.3667	0.3602	0.3439	0.355	0.3873	0.1
Q17836	0.3292	0.3172	0.3287	0.3326	0.3165	0.3433	0.3335	0.3341	0.3049	0.3652	0.3592	0.4
Q17837	0.4028	0.4303	0.3834	0.3724	0.3893	0.3791	0.3965	0.3969	0.4104	0.4022	0.4493	0.15
Q17838	0.3461	0.3254	0.303	0.2643	0.3128	0.2656	0.3513	0.2837	0.2917	0.3147	0.2587	0.5
Q17839	0.4423	0.4202	0.4467	0.3635	0.4088	0.4151	0.4332	0.4132	0.4098	0.4095	0.3786	0.15
Q17840	0.0943	0.1199	0.2081	0.1448	0.1982	0.1602	0.1724	0.1605	0.1711	0.2224	0.2168	0.0
Q17841	0.2169	0.2332	0.2025	0.2366	0.2197	0.2384	0.229	0.2153	0.2151	0.2144	0.2202	0.1
Q17842	0.4138	0.3635	0.3927	0.3587	0.4203	0.3771	0.3669	0.3711	0.3871	0.3739	0.3534	0.5
Q17843	0.3086	0.3294	0.3113	0.3525	0.3312	0.3777	0.3474	0.3451	0.3396	0.3344	0.3455	0.0
Q17844	0.3455	0.3509	0.3601	0.3242	0.3428	0.3451	0.3316	0.3741	0.3353	0.334	0.3715	0.15
Q17845	0.3122	0.3171	0.3371	0.2631	0.2851	0.293	0.2897	0.2963	0.2952	0.2908	0.2592	0.5
Q17846	0.3668	0.3457	0.4059	0.3836	0.3971	0.4219	0.4028	0.3933	0.3718	0.3728	0.4317	0.05
Q17847	0.3647	0.3244	0.3886	0.3536	0.3151	0.2992	0.3421	0.3098	0.3247	0.3593	0.3613	0.25
Q17848	0.2823	0.2991	0.3732	0.3051	0.3416	0.3032	0.3272	0.3167	0.311	0.3085	0.27	0.5
Q17849	0.2211	0.2346	0.2265	0.2022	0.2095	0.2161	0.2214	0.2033	0.2712	0.3092	0.197	0.5
Q17850	0.3721	0.3684	0.3454	0.3305	0.3126	0.3278	0.3236	0.3755	0.3269	0.3573	0.3641	0.2
Q17851	0.2105	0.208	0.2334	0.2125	0.2124	0.2065	0.2386	0.2089	0.1665	0.2041	0.1861	0.4
W60	0.2511	0.2325	0.2326	0.2382	0.2471	0.235	0.2319	0.2241	0.2317	0.2328	0.2418	0.35
W61	0.2235	0.2357	0.2252	0.2369	0.2492	0.2479	0.2429	0.2459	0.2539	0.2457	0.2554	0.0
W62	0.1822	0.2121	0.177	0.1807	0.1682	0.182	0.1827	0.1834	0.1926	0.1981	0.1773	0.2
W63	0.242	0.2425	0.2527	0.2413	0.2568	0.248	0.255	0.2544	0.2503	0.2675	0.2586	0.15

Continued on next page

Table 2: Augmentation Benefit for Multiple Levels of Generated Data α (Continued)

	$\alpha = 0$	$\alpha = 0.05$	$\alpha = 0.1$	$\alpha = 0.15$	$\alpha = 0.2$	$\alpha = 0.25$	$\alpha = 0.3$	$\alpha = 0.35$	$\alpha = 0.4$	$\alpha = 0.45$	$\alpha = 0.5$	α^*
W64	0.1895	0.1974	0.1904	0.2135	0.2076	0.2157	0.2267	0.2235	0.2222	0.2395	0.236	0.0
W65	0.2004	0.2083	0.2131	0.218	0.2275	0.228	0.2409	0.2397	0.2428	0.2429	0.2542	0.0
W66	0.167	0.1614	0.1364	0.1465	0.1358	0.1425	0.1515	0.1781	0.1509	0.1291	0.1289	0.5
W67	0.1884	0.1722	0.1742	0.1706	0.1766	0.1834	0.1878	0.1963	0.1875	0.1733	0.1816	0.15
W68	0.1813	0.1619	0.1595	0.1674	0.1683	0.1631	0.1977	0.1769	0.1643	0.1697	0.1674	0.1
W69	0.1802	0.1782	0.1819	0.1779	0.1872	0.1755	0.1776	0.1663	0.1875	0.1739	0.1774	0.35
W74	0.1875	0.1926	0.173	0.1807	0.1825	0.1786	0.1817	0.1942	0.1644	0.18	0.1778	0.4
W75	0.1608	0.1718	0.1635	0.1762	0.1669	0.1698	0.1696	0.1672	0.172	0.1645	0.1677	0.0
W77	0.046	0.1117	0.0702	0.0959	0.0666	0.0843	0.0691	0.1007	0.0845	0.0932	0.0542	0.0
W78	0.1101	0.1297	0.0936	0.1001	0.1026	0.1059	0.1236	0.1402	0.1109	0.1311	0.0974	0.1
W79	0.3106	0.3064	0.3015	0.3101	0.3199	0.3175	0.3171	0.3121	0.3112	0.296	0.3085	0.45
W80	0.3034	0.2947	0.3145	0.307	0.3104	0.314	0.3059	0.3012	0.3073	0.3119	0.3178	0.05
W81	0.2074	0.2225	0.2073	0.214	0.2055	0.2225	0.2101	0.2003	0.2149	0.2084	0.2116	0.35
W82	0.1626	0.1542	0.1671	0.1573	0.1632	0.1581	0.1536	0.1649	0.1536	0.167	0.1609	0.3
W85	0.1308	0.1138	0.13	0.1183	0.1363	0.1321	0.1138	0.1428	0.1206	0.1325	0.1367	0.05
W86	0.1274	0.1245	0.1423	0.1369	0.1266	0.119	0.1463	0.1292	0.1338	0.124	0.1144	0.5
Y15255	0.4959	0.5061	0.4615	0.4782	0.5228	0.515	0.4204	0.4963	0.4844	0.4888	0.4799	0.3
Y15256	0.4994	0.5279	0.5272	0.4957	0.5261	0.5383	0.4869	0.4644	0.4781	0.534	0.502	0.35
Y15264	0.2515	0.2832	0.3468	0.3152	0.3994	0.2923	0.2824	0.3475	0.3124	0.3696	0.3568	0.0
Y15275	0.3005	0.2751	0.3248	0.3157	0.3716	0.3502	0.3796	0.3654	0.3682	0.3956	0.3908	0.05
Y15276	0.3361	0.3806	0.3895	0.3883	0.4157	0.3895	0.4245	0.5249	0.5274	0.5498	0.5785	0.0
Y15277	0.255	0.2376	0.2422	0.2911	0.2895	0.3133	0.3587	0.2584	0.3665	0.3265	0.2662	0.05
Y15279	0.2696	0.322	0.2553	0.2916	0.3394	0.3046	0.3106	0.3244	0.3489	0.3457	0.326	0.1
Y15281	0.4057	0.4428	0.3999	0.4769	0.3973	0.4379	0.4512	0.4862	0.46	0.511	0.4577	0.2
Y15285	0.3478	0.3695	0.3354	0.3055	0.3635	0.2947	0.3253	0.293	0.3219	0.3752	0.3227	0.35
Y15286	0.3565	0.3517	0.4464	0.367	0.448	0.4026	0.4812	0.3893	0.4905	0.4617	0.4108	0.05
Y15292	0.4372	0.4531	0.415	0.4448	0.4528	0.4522	0.5137	0.446	0.4919	0.5123	0.505	0.1
Y15835	0.3805	0.4278	0.4328	0.4088	0.4195	0.4546	0.4366	0.3938	0.4788	0.4468	0.4469	0.0
Y15836	0.3741	0.3639	0.3197	0.334	0.3501	0.2727	0.3344	0.3129	0.3742	0.3689	0.3534	0.25
Y15837	0.3599	0.3103	0.328	0.321	0.3314	0.2862	0.2483	0.3055	0.3434	0.3303	0.2712	0.3
Y15838	0.2854	0.3598	0.3019	0.3099	0.2977	0.3673	0.3348	0.2973	0.347	0.316	0.3162	0.0
Y17075	0.2865	0.298	0.2681	0.2298	0.2477	0.323	0.2325	0.235	0.2808	0.1956	0.2381	0.45

Continued on next page

Table 2: Augmentation Benefit for Multiple Levels of Generated Data α (Continued)

	$\alpha = 0$	$\alpha = 0.05$	$\alpha = 0.1$	$\alpha = 0.15$	$\alpha = 0.2$	$\alpha = 0.25$	$\alpha = 0.3$	$\alpha = 0.35$	$\alpha = 0.4$	$\alpha = 0.45$	$\alpha = 0.5$	α^*
Y17124	0.1473	0.2621	0.1319	0.183	0.1815	0.1697	0.2356	0.1726	0.1625	0.2329	0.2344	0.1
Y17232	0.2947	0.3198	0.2775	0.3401	0.3313	0.3667	0.3206	0.2613	0.2938	0.317	0.3136	0.35
Y17248	0.2656	0.4149	0.4021	0.2996	0.3948	0.3037	0.4106	0.3105	0.3917	0.3384	0.3677	0.0
Y17249	0.3201	0.2936	0.2672	0.2601	0.2789	0.2881	0.2531	0.2585	0.3196	0.2945	0.2875	0.3

References

- Mohammed Ali, Mark W. Jones, Xianghua Xie, and Mark Williams. TimeCluster: dimension reduction applied to temporal data for visual analytics. *The Visual Computer*, 35(6):1013–1026, June 2019. ISSN 1432-2315. doi: 10.1007/s00371-019-01673-y. URL <https://doi.org/10.1007/s00371-019-01673-y>.
- Evgeny A Antipov and Elena B Pokryshevskaya. Interpretable machine learning for demand modeling with high-dimensional data using gradient boosting machines and shapley values. *Journal of Revenue and Pricing Management*, 19(5):355–364, 2020.
- Martin Arjovsky, Soumith Chintala, and Léon Bottou. Wasserstein GAN. *arXiv:1701.07875 [cs, stat]*, December 2017. URL <http://arxiv.org/abs/1701.07875>. arXiv: 1701.07875.
- Kasun Bandara, Hansika Hewamalage, Yuan-Hao Liu, Yanfei Kang, and Christoph Bergmeir. Improving the accuracy of global forecasting models using time series data augmentation. *Pattern Recognition*, 120:108148, 2021. ISSN 0031-3203. doi: <https://doi.org/10.1016/j.patcog.2021.108148>. URL <https://www.sciencedirect.com/science/article/pii/S0031320321003356>.
- Christoph Bergmeir, Rob J Hyndman, and José M Benítez. Bagging exponential smoothing methods using stl decomposition and box–cox transformation. *International journal of forecasting*, 32(2):303–312, 2016.
- G. E. P. Box and David A. Pierce. Distribution of Residual Autocorrelations in Autoregressive-Integrated Moving Average Time Series Models. *Journal of the American Statistical Association*, 65(332):1509–1526, December 1970. ISSN 0162-1459. doi: 10.1080/01621459.1970.10481180. URL <https://www.tandfonline.com/doi/abs/10.1080/01621459.1970.10481180>.
- Evangelos A Denaxas, Rubenka Bandyopadhyay, Dalia Patiño-Echeverri, and Nikos Pitsianis. Syntise: A modified multi-regime mcmc approach for generation of wind power synthetic time series. In *2015 Annual IEEE Systems Conference (SysCon) Proceedings*, pages 668–674. IEEE, 2015.
- J.-P Eckmann, S. Oliffson Kamphorst, and D Ruelle. Recurrence Plots of Dynamical Systems. *Europhysics Letters (EPL)*, 4(9):973–977, November 1987. ISSN 0295-5075, 1286-4854. doi: 10.1209/0295-5075/4/9/004.
- Cristóbal Esteban, Stephanie L. Hyland, and Gunnar Rätsch. Real-valued (medical) time series generation with recurrent conditional gans, 2017.
- Germain Forestier, François Petitjean, Hoang Anh Dau, Geoffrey I Webb, and Eamonn Keogh. Generating synthetic time series to augment sparse datasets. In *2017 IEEE international conference on data mining (ICDM)*, pages 865–870. IEEE, 2017.
- Rao Fu, Jie Chen, Shutian Zeng, Yiping Zhuang, and Agus Sudjianto. Time series simulation by conditional generative adversarial net, 2019.
- Aurelien Geron. *Hands-on machine learning with Scikit-Learn and TensorFlow: concepts, tools, and techniques to build intelligent systems*. O’Reilly Media, Beijing ; Boston, first edition edition, 2017. ISBN 9781491962299. OCLC: ocn953432302.
- Amirata Ghorbani and James Zou. Data shapley: Equitable valuation of data for machine learning. In *International Conference on Machine Learning*, pages 2242–2251. PMLR, 2019.
- Ian J. Goodfellow, Jean Pouget-Abadie, Mehdi Mirza, Bing Xu, David Warde-Farley, Sherjil Ozair, Aaron Courville, and Yoshua Bengio. Generative Adversarial Networks. *arXiv:1406.2661 [cs, stat]*, June 2014. URL <http://arxiv.org/abs/1406.2661>. arXiv: 1406.2661.
- Ishaan Gulrajani, Faruk Ahmed, Martin Arjovsky, Vincent Dumoulin, and Aaron Courville. Improved Training of Wasserstein GANs. *arXiv:1704.00028 [cs, stat]*, December 2017. URL <http://arxiv.org/abs/1704.00028>. arXiv: 1704.00028.
- Justin Hellermann and Stefan Lessmann. Leveraging image-based generative adversarial networks for time series generation, 2021. URL <https://arxiv.org/abs/2112.08060>.
- Nadeem Iftikhar, Xiufeng Liu, Sergiu Danalachi, Finn Ebertsen Nordbjerg, and Jens Henrik Vollesen. A scalable smart meter data generator using spark. In *OTM Confederated International Conferences" On the Move to Meaningful Internet Systems"*, pages 21–36. Springer, 2017.
- Yanfei Kang, Rob J Hyndman, and Feng Li. Gratis: Generating time series with diverse and controllable characteristics. *Statistical Analysis and Data Mining: The ASA Data Science Journal*, 13(4):354–376, 2020.
- Tero Karras, Samuli Laine, Miika Aittala, Janne Hellsten, Jaakko Lehtinen, and Timo Aila. Analyzing and improving the image quality of stylegan, 2020.

- Arthur Le Guennec, Simon Malinowski, and Romain Tavenard. Data augmentation for time series classification using convolutional neural networks. In *ECML/PKDD workshop on advanced analytics and learning on temporal data*, 2016.
- Si Woon Lee and Ha Young Kim. Stock market forecasting with super-high dimensional time-series data using convlstm, trend sampling, and specialized data augmentation. *Expert Systems with Applications*, 161:113704, 2020.
- G. M. Ljung and G. E. P. Box. On a measure of lack of fit in time series models. *Biometrika*, 65(2):297–303, 08 1978. ISSN 0006-3444. doi: 10.1093/biomet/65.2.297. URL <https://doi.org/10.1093/biomet/65.2.297>.
- Spyros Makridakis, Evangelos Spiliotis, and Vassilios Assimakopoulos. The m4 competition: Results, findings, conclusion and way forward. *International Journal of Forecasting*, 34(4):802–808, 2018.
- Leland McInnes, John Healy, and James Melville. UMAP: Uniform Manifold Approximation and Projection for Dimension Reduction. *arXiv:1802.03426 [cs, stat]*, September 2020. URL <http://arxiv.org/abs/1802.03426>. arXiv: 1802.03426.
- Luke Merrick and Ankur Taly. The explanation game: Explaining machine learning models using shapley values. In *International Cross-Domain Conference for Machine Learning and Knowledge Extraction*, pages 17–38. Springer, 2020.
- George Papaefthymiou and Bernd Klockl. Mcmc for wind power simulation. *IEEE transactions on energy conversion*, 23(1):234–240, 2008.
- Thomas Schreiber and Andreas Schmitz. Surrogate time series. *Physica D: Nonlinear Phenomena*, 142(3): 346–382, 2000. ISSN 0167-2789. doi: [https://doi.org/10.1016/S0167-2789\(00\)00043-9](https://doi.org/10.1016/S0167-2789(00)00043-9). URL <https://www.sciencedirect.com/science/article/pii/S0167278900000439>.
- Lloyd S. Shapley. Notes on the N-Person Game — II: The Value of an N-Person Game. Technical report, RAND Corporation, August 1951. URL https://www.rand.org/pubs/research_memoranda/RM0670.html.
- Slawek Smyl and Karthik Kuber. Data preprocessing and augmentation for multiple short time series forecasting with recurrent neural networks. In *36th International Symposium on Forecasting*, 2016.
- James Theiler, Stephen Eubank, André Longtin, Bryan Galdrikian, and J Doyne Farmer. Testing for nonlinearity in time series: the method of surrogate data. *Physica D: Nonlinear Phenomena*, 58(1-4):77–94, 1992.
- Zhiguang Wang and Tim Oates. Encoding time series as images for visual inspection and classification using tiled convolutional neural networks. 2014.
- L. Wyse. Audio Spectrogram Representations for Processing with Convolutional Neural Networks. *arXiv:1706.09559 [cs]*, June 2017. URL <http://arxiv.org/abs/1706.09559>. arXiv: 1706.09559.
- Jinsung Yoon, Daniel Jarrett, and Mihaela van der Schaar. Time-series generative adversarial networks. In H. Wallach, H. Larochelle, A. Beygelzimer, F. d'Alché-Buc, E. Fox, and R. Garnett, editors, *Advances in Neural Information Processing Systems*, volume 32. Curran Associates, Inc., 2019. URL <https://proceedings.neurips.cc/paper/2019/file/c9efe5f26cd17ba6216bbe2a7d26d490-Paper.pdf>.
- Yuyu Yuan, Wen Wen, and Jincui Yang. Using data augmentation based reinforcement learning for daily stock trading. *Electronics*, 9(9):1384, 2020.
- Xiang Zhang, Junbo Zhao, and Yann LeCun. Character-level convolutional networks for text classification. *Advances in neural information processing systems*, 28:649–657, 2015.
- Liu Ziyin, Kentaro Minami, and Kentaro Imajo. What data augmentation do we need for deep-learning-based finance? *arXiv preprint arXiv:2106.04114*, 2021.